# Propagation and attenuation of pseudo surface acoustic modes at the (111) face of a GaAs crystal studied by Brillouin spectroscopy

V.V. Aleksandrov and M.V. Saphonov
*Chair for Crystallophysics, Physics Department, Moscow State University, Moscow 117234, Russia*

V.R. Velasco
*Instituto de Ciencia de Materiales, Consejo Superior de Investigaciones Científicas, Serrano 123, 28006 Madrid, Spain*

(Received 26 April 1994)

Acquisition of Brillouin spectra for light scattered by the (111) free surface of GaAs provides the experimental determination of pseudo-surface-mode velocities and their attenuation for all nonequivalent azimuthal in-plane directions. Observations were performed with *p-p* and *p-s* polarization configurations. Good agreement between measured and calculated velocities of the pseudo surface modes is achieved. A reasonable correlation between the azimuthal behavior of the pseudo-surface-mode attenuation and that of the linewidth of the Brillouin satellites corresponding to these modes is obtained.

## I. INTRODUCTION

The study of the acoustical properties of the surfaces of anisotropic crystals shows that in addition to the normal surface elastic wave of Rayleigh type, called in those cases generalized surface waves (GSW's), pseudo surface modes (PSM's) can also exist.[1] These modes radiate energy into the bulk as they propagate along the surface and have a velocity ($V_{\mathrm{PSM}}$) such that $V_{\mathrm{STW}} < V_{\mathrm{PSM}} < V_{\mathrm{FTW}}$. Here $V_{\mathrm{FTW}}$ is the velocity of a fast transverse bulk wave for the same azimuthal direction in the surface plane, and $V_{\mathrm{STW}}$ is the slow transverse bulk wave. The properties of the PSM's depend on different variables associated to the symmetry of the crystal, the surface orientation, and the propagation direction of the wave. For many known cases the radiating term is small enough so that the PSM's satisfy most of the experimental conditions for the surface waves and can be detected in ultrasonic experiments.[2] On the other hand, both Brillouin scattering experiments,[3–5] and calculations of the density of phonon modes at the surface[6–8] put in evidence the density peak maxima at $V = V_{\mathrm{PSM}}$ at thermal equilibrium, satisfying the conditions of the existence of a PSM as stated in Ref. 1.

These spectral singularities should be attributed to the behavior of the reflection coefficients of the bulk waves at the crystal-vacuum boundary providing the intense shear bulk phonon scattering for the directions of nearly in-plane wave vector orientation.[9] From this point of view PSM resonances in the equilibrium phonon density distribution represent a group of Lamb waves of particularly large amplitude of vibration in the case when the plate thickness becomes infinite.[3,9,10]

PSM's density maxima can be also considered as surface phonons having a finite lifetime and decaying into the bulk phonons.[5,8] In this scheme the widths of PSM peaks give the lifetimes of the corresponding pseudo surface states and thus describe the PSM attenuation and its "leakage." In light scattering experiments this should affect the linewidths of corresponding Brillouin satellites and this could be experimentally identified.

Brillouin scattering has proved to be a very powerful experimental technique to study the surface modes in the GHz range.[11] Some recent works have shown its potential for the investigation of the PSM's.[5,12–16] Measurements of the linewidths of the Brillouin satellites corresponding to a PSM ($\delta f_{\mathrm{PSM}}$) have been conducted in cubic crystals of $z$ cut having elastic anisotropy ratio $\mu = 2C_{44}/(C_{11} - C_{12}) > 1$ (Si, Ge, GaAs, InSb).[12] They exhibited nonmonotonous azimuthal behavior of $\delta f_{\mathrm{PSM}}$ similar to that of the PSM attenuation curve, where $C_{ij}$ are the elastic constants. $\delta f_{\mathrm{PSM}}$ presents its minimal values for the azimuthal directions parallel to $[1\bar{1}0]$ where the PSM leakage goes down to zero and it degenerates into the normal surface mode. $\delta f_{\mathrm{PSM}}$ becomes minimal once again for directions rotated from $[1\bar{1}0]$ by 18° (Si), 19° (Ge), 22° (GaAs), and 23° (InSb), where a PSM wave vector confines the surface for the second time.[17,18] Similar $\delta f_{\mathrm{PSM}}$ registrations were also performed for (110) surfaces of PbTe crystals having $\mu < 1$.[14]

The aim of the present paper is the experimental study of the behavior of the PSM's at the (111) surface of cubic crystals with $\mu > 1$. Then we shall be able to describe the features of the PSM's propagation together with the PSM attenuation. The Brillouin surface light scattering technique was used for this purpose, together with theoretical calculations of the long wave phonon density of states at the surface. In Sec. II we present the experimental techniques and some brief comments on the theoretical methods employed. Section III contains the experimental results and the discussion, and conclusions are presented in Sec. IV.

 

## II. EXPERIMENTAL TECHNIQUES AND THEORETICAL METHODS

For cubic crystals with $\mu > 1$, the character of the displacements of PSM's at (111) free surface and their azimuthal variation are substantially different from those corresponding to the samples of $z$ cut. The presence of a mirror symmetry in the latter case causes mainly a sagittal orientation for PSM displacements for nearly all azimuthal directions with a PSM. This confines regular surface Brillouin scattering observation conditions, i.e., $p$-$p$ scattering configuration, where the first index corresponds to the polarization of the incident light beam and the other to the scattered one. Thus it will be sensitive to shear vertical surface excitations via a ripple scattering mechanism,[19] and to longitudinal ones via subsurface elasto-optic coupling.[7]

In the case of (111) free surfaces the absence of mirror symmetry causes that PSM amplitudes are of a mixed nature, having strong shear horizontal contribution for most azimuthal directions in the plane. The shear horizontal contribution becomes the main component of the amplitude if one leaves the $[1\bar{1}0]$ azimuthal direction ($\theta = 0°$) moving towards $[1\bar{2}1]$ ($\theta = 30°$). At $\theta = 30°$ the PSM is transformed into the bulk mode satisfying stress-free boundary conditions and having purely shear horizontal amplitude, also called exceptional bulk mode. Registration of shear horizontal surface excitations cannot be performed using the conventional $p$-$p$ surface Brillouin scattering scheme. They become "visible" only with a $p$-$s$ (or $s$-$p$) scattering configuration via elasto-optic subsurface coupling.[7,20] However, one should keep in mind that the effectiveness of elasto-optic coupling is strongly limited by the depth of the subsurface scattering volume which should be reasonably small. This depth limitation is required to achieve a successful detection of the surface contribution to the light scattering, because we must be able to discriminate the former contribution from that coming from the traditional bulk scattering.[21] These controversial requirements, i.e., weak bulk scattering contribution but still effective subsurface elasto-optic coupling, strongly specify the optical properties of the samples in which shear horizontal surface excitations may be observed.

Here we use GaAs crystals for which the registration of exceptional bulk modes with purely shear horizontal amplitudes in the case of (111) free surfaces have been recently communicated.[20] The observation of Brillouin components of light scattered by (111) free surface excitations of PSM type in GaAs crystals in the range $0° \leq \theta \leq 20°$ was performed in Refs. 5 and 13, a $p$-$p$ configuration scheme being applied. However, no experiments on corresponding pseudo surface phonon state lifetime determination have been conducted yet.

Surface Brillouin scattering spectra were taken with a five pass piezo scanned Fabry-Perot interferometer of Burleigh. Measurements were conducted in the backscattering geometry using 50–75 mW of single mode $\lambda = 514.5$ nm line of an $Ar^+$ ion laser (Spectra Physics 165-03), see also Ref. 22. In all the experiments the electric vector **E** of the incident beam was parallel to the plane of incidence, the polarization of the scattered light being specified according to the experiment, i.e., $p$-$p$ and $p$-$s$ scattering configurations. We chose 25.3 GHz free spectral range for our investigations because it enables us to resolve Brillouin components corresponding to a GSW and to a PSM for all the azimuthal directions in the (111) plane, working finesse being equal to 60. The angle of incidence of light $\alpha$ for different observations with a $p$-$p$ scattering configuration was varied from 50° to 70°. For the experiments with a $p$-$s$ scattering configuration the range $45° \leq \theta \leq 55°$ was used in order to maximize the contribution of the shear horizontal displacements cross section.[7,20]

Specially prepared low dislocation specimens of GaAs with highly smoothed (111) faces were used in our investigations. Misorientation of the working surfaces was controlled by x-ray measurements and did not exceed 1.5°.

Two theoretical approaches have been used to describe the surface excitations. One follows the scheme of Ref. 1 of solving the equations of motion and the boundary conditions extending normal surface calculations to the PSM's. This implies the introduction of an imaginary part of the velocity (frequency) which allows for a direct search of the PSM velocity values and its attenuation. The second one is based on surface Green function matching method[8,23] and is applied to the calculation of the entire surface excitation spectrum. It allows one to obtain GSW as well defined peaks at $V < V_{\mathrm{STW}}$ and PSM's as resonances in the continuum of phonon states at $V \geq V_{\mathrm{STW}}$.

The velocities obtained by both theoretical methods are always the same. However, the procedure of the evaluation of pseudo surface state lifetime from the PSM power spectrum resonance linewidth using a simple Lorentzian best fit similar to that of Refs. 5, 12, and 14 has to be improved. Contrary to the systems considered in these references the original PSM resonances for the (111) free surface of cubic crystals have an asymmetric shape. Let us illustrate this by a spectrum of longitudinal surface excitations for the $[1\bar{1}0]$ azimuthal direction ($\theta = 0°$), see Fig. 1, in which the asymmetry appears in the low velocity (frequency) part. This asymmetry produces a 6% mismatch between the results of calculations of PSM attenuation following the scheme of Ref. 1 and the simple Lorentzian PSM lifetime best fit.

According to formal scattering theory resonances can be viewed as distortions of the density of states in the continuum of scattering states.[24] In the vicinity of the values of the frequencies of the resonant modes the change in the density of states can be described by a Lorentzian peak. In real cases this peak will show itself in the total change of the density of states superimposed to the continuum of scattering states and thus can lose its perfect Lorentzian shape, as illustrated in Fig. 1(a). It is then clear that we can follow the description given above and decompose the asymmetric peak in separate contributions. Thus we vary both (i) the shape of the continuum part of the spectra, responsible for nonresonant bulk phonon scattering at the crystal-vacuum boundary, in the vicinity of $V_{\mathrm{PSM}}$, by means of a smooth continuation [grey bold line in Fig. 1(b)]; (ii) the Lorentzian

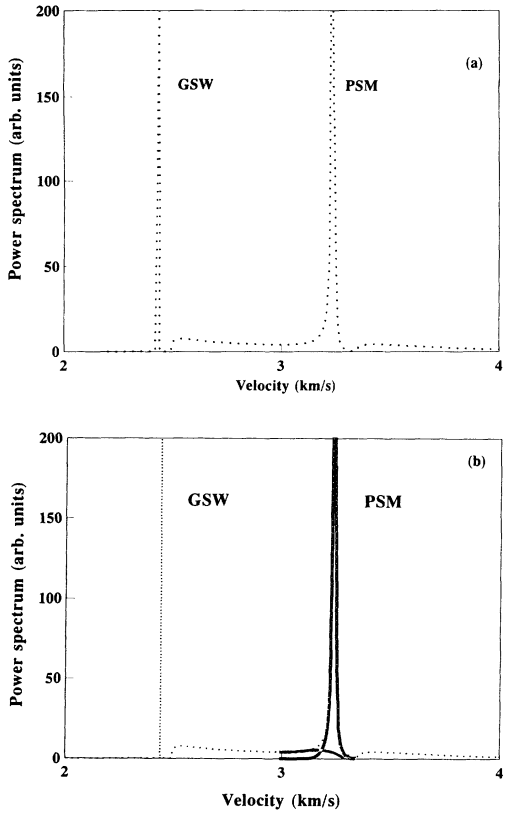


FIG. 1. Power spectrum of longitudinal surface excitations in GaAs crystal of (111) cut. The propagation angle $\theta$ measured from the [110] crystallographic direction is equal to 0°. The original spectrum is shown in (a) and (b) by a dotted curve. The results of best fit modeling of the original spectrum by a truly Lorentzian peak and the continuum nonresonance part of the spectra are shown in (b) by black and grey bold lines, respectively.

curve (linewidth and height) corresponding to the PSM [bold black line in Fig. 1(b)]. Following this procedure the attenuation mismatch can be drastically reduced, becoming practically negligible. The elastic data used in these and all the other calculations are given in Table I.

The experimental attenuation of the PSM was evaluated from Brillouin satellite linewidths by use of special deconvolution procedures based on the algorithms of Ref. 25. Due to insufficient spectral resolution in the experiments and a systematic broadening of the Brillouin lines related to a finite scattered light acceptance aperture we were not able to make the absolute measurements of the PSM attenuation. Meanwhile, the spectral components of light relating to the PSM were found to be intense enough to make proper qualitative linewidth comparisons for both scattering configurations, *p-p* and *p-s*, similar to those conducted by us earlier for the *p-p* configuration in Refs. 12, 14, and 16.

## III. EXPERIMENTAL RESULTS AND DISCUSSION

Figure 2 represents Brillouin spectra registered at $\theta = 0°$ for the *p-p* scattering configuration [Fig. 2(a)], and for the *p-s* one [Fig. 2(b)], see the dots. Here Brillouin frequency shifts $\delta f$ are also given in velocity units, $V = \delta f \lambda/[2\sin(\alpha)]$. The presence of a Brillouin satellite background in the figure is due to light scattering data accumulation conditions.

The reference power spectrum of the surface displacement is also shown, see Fig. 2(c). It is seen from Fig. 2(c) that both surface excitations, GSW's and PSM's, being characterized by corresponding density peaks, show all the components of the displacements, i.e., longitudinal (dotted line), shear vertical (solid line), and shear horizontal (dashed line). A mixed type of GSW and PSM amplitudes leads to the registration of both surface excitations for both scattering configurations, for *p-p* scattering (shear vertical surface displacements, ripple mechanism, and longitudinal surface displacements, subsurface elasto-optic coupling), see Fig. 2(a), and for *p-s* scattering (shear horizontal surface displacements, subsurface elasto-optic coupling), see Fig. 2(b).

The weaker (approximately 20 times) intensity of the Brillouin satellites in the case of the *p-s* configuration scheme should be remarked. The latter can be explained by the adequate proportion between *p-p* and *p-s* light scattering cross sections.

Theoretical cross sections are shown in Figs. 2(a) and 2(b) by solid lines. They were calculated according to Ref. 7 by means of the surface power spectra of Fig. 2(c) convoluted with the instrumental function of the interferometer. The refractive index necessary for the evaluations is tabulated. Reasonable agreement between experimental data and cross section is observed for the entire frequency region for both *p-p* and *p-s* scattering spectra.

Brillouin spectra of a GaAs crystal for an azimuthal direction of $\theta = 20°$ are shown in Fig. 3. The spectrum of light taken at the *p-p* scattering configuration is shown in Fig. 3(a), and that of the *p-s* one is shown in Fig. 3(b). Figure 3(c) completes the experimental data of Figs. 3(a)and 3(b) by showing the results of surface

TABLE I. Values of elastic moduli, mass density, and dielectric function parameters of GaAs used in the calculations

| Elastic constants[a] $10^{11}$ (N/m$^2$) | | | Elasto-optic constants[b] | | | Dielectric function[b] | Mass density[a] (kg/m$^3$) |
|---|---|---|---|---|---|---|---|
| $C_{11}$ | $C_{12}$ | $C_{44}$ | $k_{11}$ | $k_{12}$ | $k_{44}$ | $\epsilon_0$ | $\rho_0$ |
| 1.888 | 0.538 | 0.585 | 42.5 | 51.0 | 25.5 | 18 | 5230.0 |

[a]Reference 26.
[b]Reference 7.

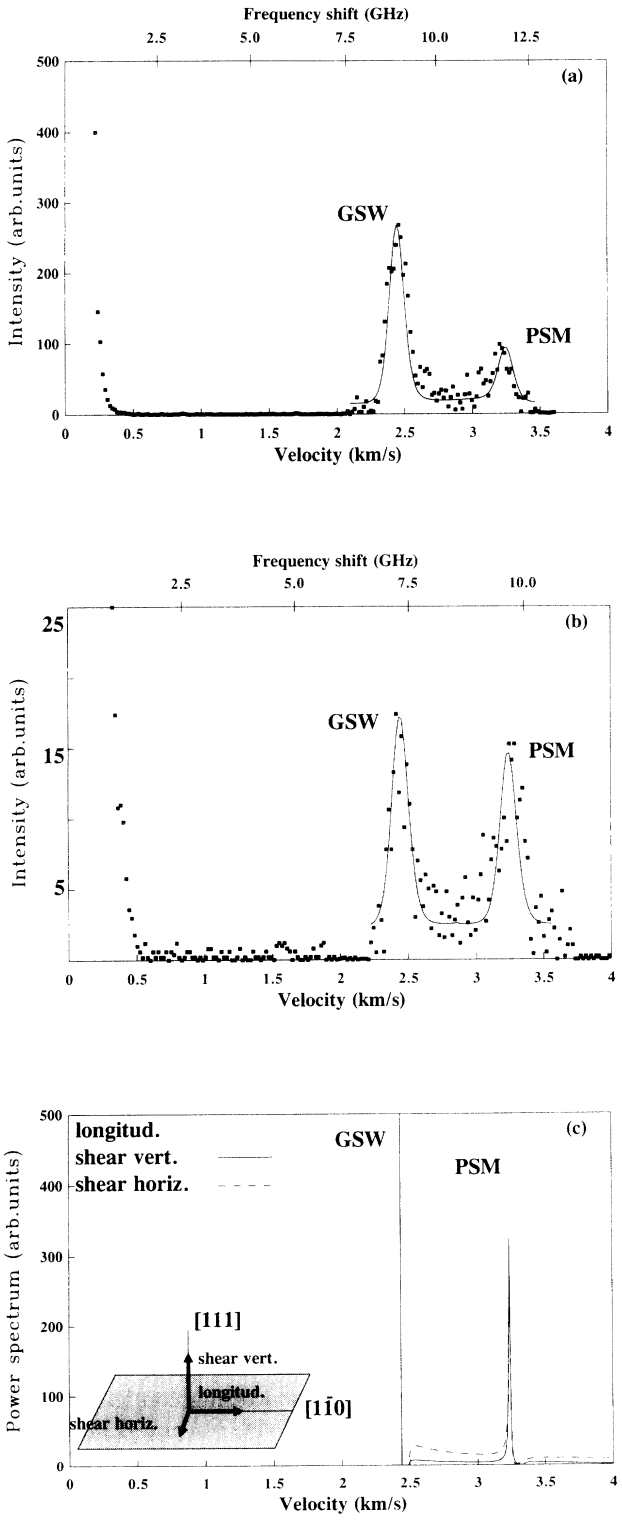


FIG. 2. Spectra of light scattered by (111) free surface of GaAs crystal at $\theta = 0°$ for $p$-$p$ (a) and $p$-$s$ (b) scattering configurations. Experimental data are marked by dots and the theoretical cross sections are shown by solid curves. The reference calculated spectrum of surface excitations is represented in (c), displacement orientations being illustrated in the inset. All the spectra peaks corresponding to generalized surface wave and pseudo surface mode are labeled as GSW and PSM, respectively.

phonon density calculations for a different type of displacements.

It is seen from Fig. 3 that with variation of $\theta$ from 0° to 20° the GSW displacements become more sagittal-like, and this produces the increase in Brillouin satellite intensity related to the GSW for the $p$-$p$ scattering configuration. On the contrary, the PSM polarization

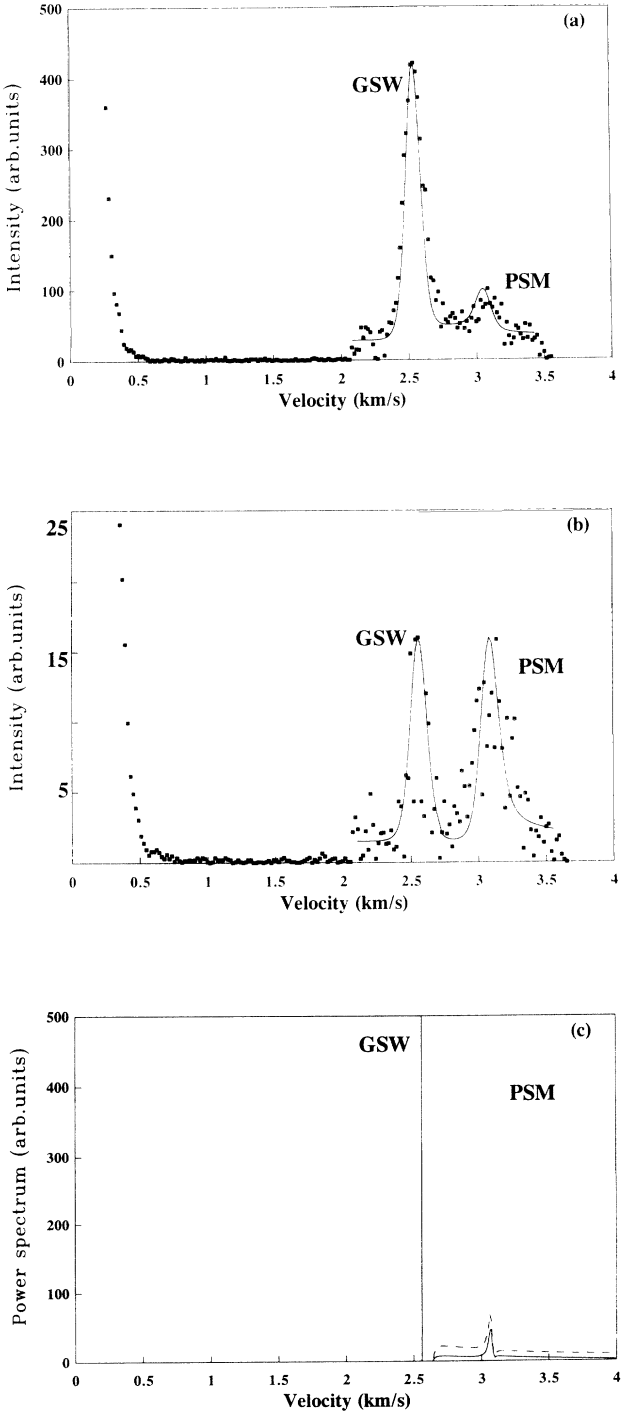


FIG. 3. Spectra of light scattered by (111) free surface of GaAs crystal at $\theta = 20°$. The same conventions as in Fig. 2.

is becoming more shear horizontal and the intensity of its Brillouin line tends to decrease for the *p-p* configuration and to increase for the *p-s* configuration. As in the previous case the theoretical cross section reasonably fits the experimental points for both spectra represented in Figs. 3(a)and 3(b).

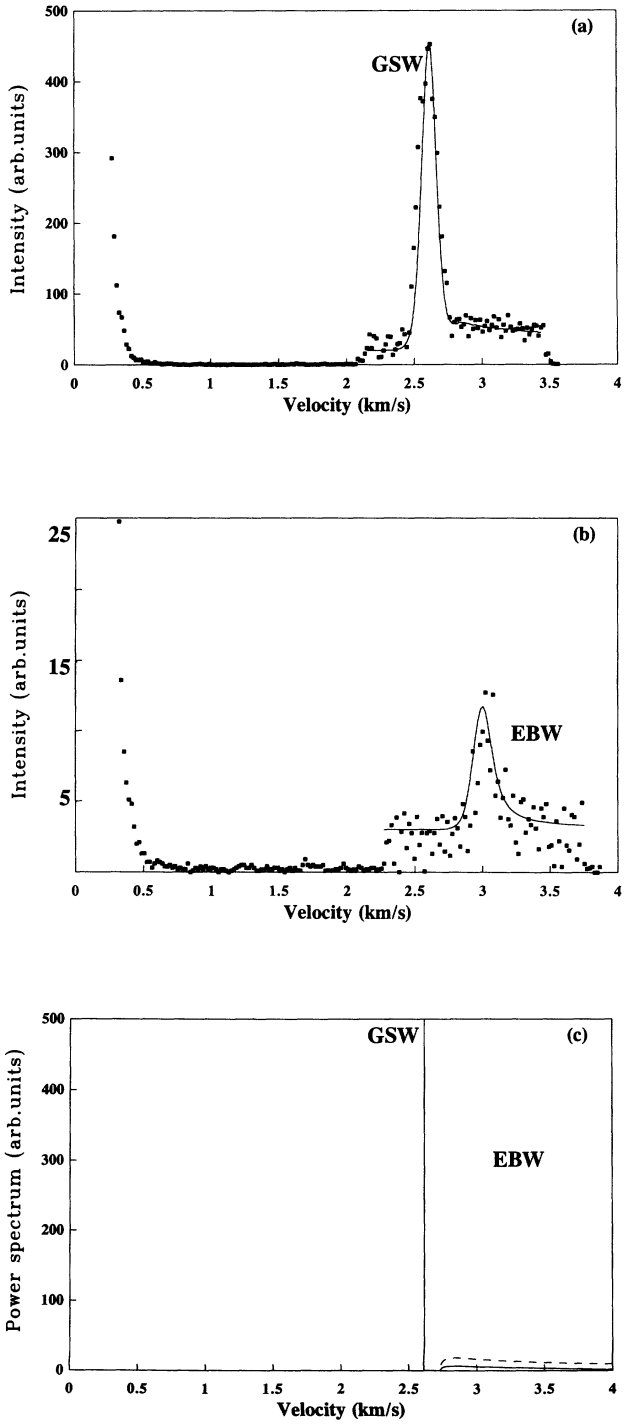


FIG. 4. Spectra of light scattered by (111) free surface of GaAs crystal at $\theta = 30°$. The same conventions as in Fig. 2. Peaks corresponding to exceptional bulk mode are labeled in (b) and (c) spectra as EBW.

At $\theta = 30°$ (azimuthal direction parallel to $[1\bar{2}1]$) the GSW displacement ellipse lies in the sagittal plane thus producing further intensity growth of the corresponding Brillouin satellite for *p-p* scattering, and the disappearance of that Brillouin line for the *p-s* configuration. The single satellite registered in the latter observation conditions relates with the exceptional bulk wave of purely horizontal polarization into which the PSM is transformed. The high velocity (frequency) broadening of the GSW Brillouin line observed in the experimental spectra in Fig. 4(a) is uniquely caused by the presence of the continuum of phonon states for $V \geq V_{STW}$ having shear vertical character and contributing to the scattered light spectral content via the ripple scattering mechanism.

The dependence of phase velocities of bulk (STW and FTW) and surface waves (GSW and PSM) on the prop-

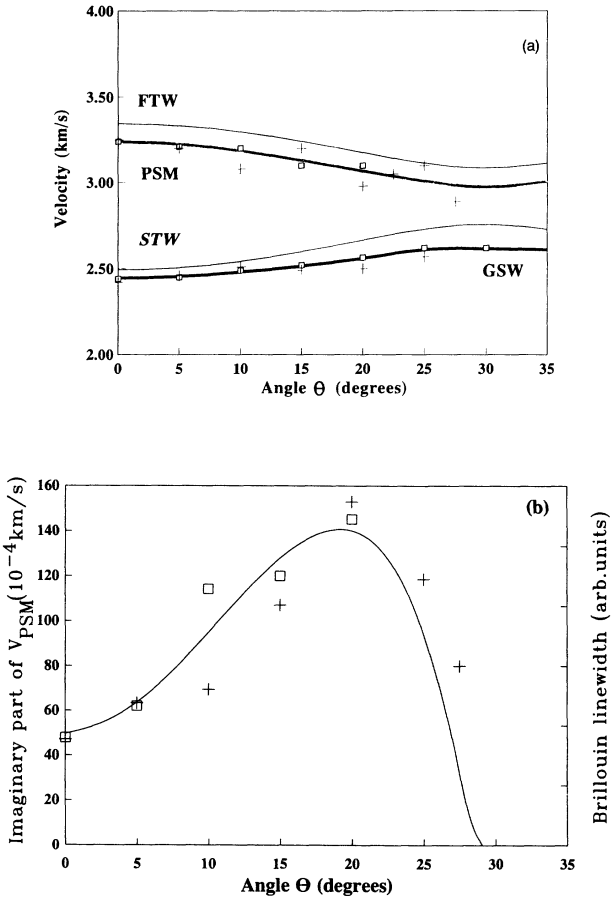


FIG. 5. (a) Phase velocities of bulk and surface modes on the (111) surface on GaAs, versus propagation angle $\theta$. The calculated dispersions for FTW, STW bulk waves are shown by the black bold line, and for PSM by the grey bold line. The experimental data for GSW and for PSM are marked by squares and crosses for *p-p*, and for *p-s* configuration schemes, respectively. (b) Attenuation of the PSM vs $\theta$. The theoretical curve represents the imaginary part of $V_{PSM}$. The crosses and squares are the results of Brillouin linewidth measurements represented in arbitrary units. The same conventions as in (a).

agation direction is given in Fig. 5(a). Solid curves correspond to the calculated $V_{STW}$ and $V_{FTW}$ values. The bold lines represent GSW and PSM theoretical velocity values. Experimentally determined GSW and PSM velocities are shown as squares for *p-p* scattering and as crosses for *p-s* scattering. In both scattering configurations experimental velocity values were defined as the positions of the maxima of the observed Brillouin peaks. These values were further improved by optimization of the position of the maxima by deconvolution best fitting.

One can find a good correlation between surface waves theoretical curves (GSW and PSM) and corresponding experimental velocity values obtained from Brillouin scattering data for both configuration schemes, deviations between experimental and theoretical values being $\approx 2\%$ for the *p-p* scattering configuration and $\approx 5\%$ for the *p-s* one. The larger discrepancy between experimental and theoretical velocity values for *p-s* scattering is explained by a weaker Brillouin component intensity character associated to this configuration, together with problems of increasing noise during long term data accumulation periods.

The PSM attenuation given by the imaginary part of the velocity (frequency) is shown in Fig. 5(b) by a solid curve. Corresponding linewidths of Brillouin lines after deconvolution are shown in the arbitrary scale, right ordinate axis. The linewidths measured for *p-p* and *p-s* configurations have the same symbols as in Fig. 5(a).

Qualitative agreement between variation of the linewidths of PSM Brillouin satellites and the character of the attenuation curve is observed for both scattering configurations. Experimental errors are of the order of 10–15% for the *p-p* configuration and of the order of 20% for the *p-s* one. The larger linewidth discrepancy for the *p-s* scheme has the same origin as was previously discussed for the velocity determinations. In spite of the higher experimental error, the *p-s* configuration plays an important role in accumulating linewidth data in the whole $\theta$ span, and especially for $20° \leq \theta \leq 30°$.

## IV. CONCLUSIONS

In the range $0° \leq \theta \leq 20°$ surface excitation spectra show PSM resonances for shear vertical and longitudinal displacements evidenced in Brillouin experiments with a *p-p* scattering configuration. In order to describe the PSM behavior for the whole range of (111) plane azimuthal directions, the *p-s* scattering configuration sensitive to shear horizontal surface displacements was used.

Registration of Brillouin spectra for both scattering configurations, *p-p* and *p-s* schemes, enables us to determine experimentally the PSM velocities and their attenuation for all nonequivalent directions in the range $0° \leq \theta \leq 30°$. Good agreement between measured and calculated values of $V_{PSM}$ is obtained. Reasonable correlation between the azimuthal behavior of the PSM attenuation represented by the imaginary part of the PSM velocity curve and that of the linewidth of PSM corresponding Brillouin satellites is also found.

## ACKNOWLEDGMENTS

The authors are thankful to M.S.A.V. Gladkevitch for his help with the calculations, Dr. V.M. Avduihina for a perfect GaAs sample, Dr. V.G. Mozhaev, and Professor F. García-Moliner for fruitful discussions, and Professor I.A. Yakovlev and Dr. T.S. Velichkina for their interest in our work. The contribution of V.V.A. and V.R.V. was partially supported by NATO under Collaborative Research Grant No. 930164.

[1] G.W. Farnell, in *Physical Acoustics*, edited by W.P. Mason and R.N. Thurston (Academic Press, New York, 1970), Vol. VI, p. 109.
[2] See, for example, F.R. Rollins, T.C. Lim, and G.W. Farnell, Appl. Phys. Lett. **12**, 236 (1968).
[3] J.R. Sandercock, Solid State Commun. **26**, 547 (1978).
[4] V.V. Aleksandrov, T.S. Velichkina, V.G. Mozhaev, and I.A. Yakovlev, Solid State Commun. **77**, 559 (1991).
[5] G. Carlotti, D. Fioretto, L. Giovannini, F. Nizzoli, G. Socino, and L. Verdini, J. Phys. Condens. Matter **4**, 257 (1992).
[6] V. Bortolani, F. Nizzoli, and G. Santoro, J. Phys. F **8**, L215 (1978).
[7] A.M. Marvin, V. Bortolani, and F. Nizzoli, J. Phys. C **13**, 299 (1980); A.M. Marvin, V. Bortolani, F. Nizzoli, and G. Santoro, *ibid.* **13**, 1607 (1980).
[8] V.R. Velasco and F. García-Moliner, J. Phys. C **13**, 2237 (1980).
[9] B.A. Auld, *Acoustic Waves and Field in Solids* (Wiley, New York, 1973), Vols. I and II.
[10] R.E. Camley and F. Nizzoli, J. Phys. C **18**, 4795 (1985).
[11] See the review, F. Nizzoli and J.R. Sandercock, in *Dynamical Properties of Solids*, edited by G.K. Horton and A.A. Maradudin (North-Holland, Amsterdam, 1990), Vol. 6, p. 281.
[12] V.V. Aleksandrov, T.S. Velichkina, Ju.B. Potapova, and I.A. Yakovlev, Phys. Lett. A **171**, 103 (1992); see also, V.V. Aleksandrov, T.S. Velichkina, V.G. Mozhaev, Ju.B. Potapova, A.K. Khmelev, and I.A. Yakovlev, *ibid.* **162**, 418 (1992).
[13] V.V. Aleksandrov, T.S. Velichkina, Yu.B. Potapova, and I.A. Yakovlev, Zh. Eksp. Teor. Fiz. **102**, 1891 (1992) [JETP **75**, 1018 (1992)].
[14] V.V. Aleksandrov, T.S. Velichkina, P.A. Vorob'ev, Yu.B. Potapova, and I.A. Yakovlev, Zh. Eksp. Teor. Fiz. **103**, 2170 (1993) [JETP **76**, 1085 (1993)].
[15] V.V. Aleksandrov, C.E. Bottani, G. Caglioti, G. Ghislotti, C. Marinoni, P. Mutti, N.L. Yakovlev, and N.S. Sokolov, J. Phys. **6**, 1947 (1994).
[16] V.V. Aleksandrov, M.V. Saphonov, V.R. Velasco, N.L. Yakovlev, and L.Ph. Martynenko, J. Phys. Condens. Matter **6**, 3347 (1994).
[17] G.I. Stegeman, J. Appl. Phys. **47**, 1712 (1976).
[18] R.M. Taziev, Akust. Zh. **33**, 157 (1987) [Sov. Phys. Acoust.

**33**, 100 (1987)].
[19] R. Loudon, J. Phys. C **11**, 2623 (1978).
[20] V.V. Aleksandrov and A.V. Gladkevitch, J. Phys. Condens. Matter **6**, 3359 (1994).
[21] I.L. Fabelinsky, *Molecular Light Scattering of Light* (Plenum Press, New York, 1968).
[22] V.V. Aleksandrov, T.S. Velichkina, V.I. Voronkova, A.M. Diakonov, P.P. Syrnikov, I.A. Yakovlev, and V.K. Yanovskii, Phys. Lett. A **142**, 307 (1989).
[23] F. García-Moliner, Ann. Phys. (Paris) **2**, 179 (1977); F. García-Moliner and V. R. Velasco, *Theory of Single and Multiple Interfaces* (World Scientific, Singapore, 1992).
[24] F. García-Moliner, *Theory of Imperfect Crystalline Solids, Trieste Lectures 1970* (IAEA, Vienna, 1971), p. 1.
[25] S.M. Lindsay, S. Burgess, and I.W. Shepherd, Appl. Optics **16**, 1404 (1977).
[26] A.J. Slobodnik Jr., E.D. Conway, and R.T. Delmonico, *Microwave Acoustics Handbook*, Surface Wave Velocities Vol. 1A (Air Force Cambridge Research Laboratories, Hanscom AFB, MA, 1973).